Check for updates

Kinetic modeling of microwave-assisted esterification for biofuel additive production: conversion of levulinic acid with pentanol using Dowex® 50WX8 catalyst

Luis A. Gallego-Villada[1] · **Edwin A. Alarcón**[1] · **Ángel G. Sathicq**[2] · **Gustavo P. Romanelli**[2]
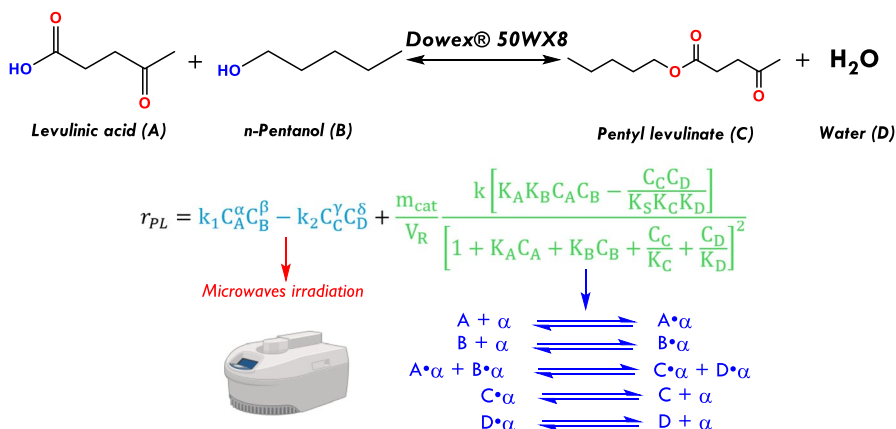
© The Author(s) 2024

Abstract

This study explores the esterification of levulinic acid with 1-pentanol, employing Dowex® 50WX8 as a catalyst under microwave irradiation. Key parameters such as the pentanol/acid molar ratio, temperature, and catalyst loading were evaluated and utilized for kinetic modeling. The kinetic behavior of the reaction was investigated using a dual-model approach: a pseudo-homogeneous model to account for the microwave effect and catalytic contributions modeled through LHHW and Eley–Rideal mechanisms. The best model was chosen based on statistical results obtained from Markov Chain Monte Carlo (MCMC) analysis, which involved an LHHW model with the surface reaction as the limiting step, resulting in an activation energy of 50.6 kJ mol^{-1} for the catalytic synthesis of pentyl levulinate. The role of the alcohol in the esterification route was explained, and catalytic stability was confirmed, with the catalyst maintaining activity over multiple cycles. The absence of mass transfer limitations was proved using the Weisz–Prater criterion. A plausible reaction pathway was proposed for the levulinic acid esterification over the 50WX8 catalyst.

✉ Luis A. Gallego-Villada
  alfonso.gallego@udea.edu.co

1 Environmental Catalysis Research Group, Chemical Engineering Faculty, Universidad de Antioquia, Medellín, Colombia

2 Centro de Investigación y Desarrollo en Ciencias Aplicadas "Dr. Jorge J. Ronco" CINDECA, (CONICET-CIC-UNLP), Facultad de Ciencias Exactas, Universidad Nacional de La Plata, Calle 47 No 257, B1900AJK La Plata, Argentina

 Springer

Graphical abstract

Levulinic acid (A)   n-Pentanol (B)   Dowex® 50WX8   Pentyl levulinate (C)   Water (D)

$$r_{PL} = k_1 C_A^\alpha C_B^\beta - k_2 C_C^\gamma C_D^\delta + \frac{m_{cat}}{V_R} \frac{k\left[K_A K_B C_A C_B - \frac{C_C C_D}{K_S K_C K_D}\right]}{\left[1 + K_A C_A + K_B C_B + \frac{C_C}{K_C} + \frac{C_D}{K_D}\right]^2}$$

Microwaves irradiation

$$
\begin{aligned}
A + \alpha &\rightleftharpoons A{\bullet}\alpha \\
B + \alpha &\rightleftharpoons B{\bullet}\alpha \\
A{\bullet}\alpha + B{\bullet}\alpha &\rightleftharpoons C{\bullet}\alpha + D{\bullet}\alpha \\
C{\bullet}\alpha &\rightleftharpoons C + \alpha \\
D{\bullet}\alpha &\rightleftharpoons D + \alpha
\end{aligned}
$$

Introduction

Levulinic acid (LA) is among twelve chemicals derived from lignocellulosic material for energy applications like biofuel production. LA offers versatility in transformations due to its structure's two functional groups such as carbonyl and carboxyl. Still, esterification reactions to obtain alkyl levulinates are of great interest because their properties are suitable for blending with fossil fuels [1] and alkyl C_4–C_{10} are under study for their better solubility and other compatible properties [2]. Some catalytic systems have been studied with acid heterogeneous catalysts like zeolites and modified mesoporous materials with a typical yield of 80% or higher [1]. Esterification of LA with pentanol has not been widely reported [2–5]; immobilized lipase reported a conversion of 99%. PW12 supported MCM-22 produced 67% yield with 96% selectivity; catalysts such as organocatalyst CX4SO₃H, calix[4]arene, in the presence of microwave, and polystyrene resin modified with –SO₃H under flow showed yields to pentyl levulinate near 100%. In fact, microwaves have attracted the attention of heterogeneous catalysis due to the reduction in reaction times and the possibility of better selectivity concerning conventional heating [6]. Methyl levulinate was produced by esterification and microwave irradiation in the presence of potassium salts with a yield of 90% [7].

Dowex® 50WX8 is a strongly acidic resin with diverse applications. It has been used in adsorption [8–13], esterification reactions such as propionic acid with 1-propanol [14], acetic acid with isobutanol [15], butyric acid with butyl alcohol [16], lactic with ethanol [17], and castor oil with 2-ethylhexanol [18]. This commercial catalyst looks promise due to its suitable acidity for the esterification reaction of

levulinic acid, yielding pentyl levulinate, which is valuable for various applications, including plasticizing agents [19], fragrance chemicals [20], solvents [21], and as intermediates in organic process industries [21]. Moreover, its potential as an oxygenated additive for diesel and other fuels is particularly noteworthy [21–23], significantly enhancing the fuel properties [24]. Levulinate esters have been demonstrated to effectively reduce greenhouse gas emissions [25, 26]. In diesel, the addition of levulinate ester has been shown to decrease NO_x and SO_x emissions [26].

Kinetics is important for reactor analysis and design [27]. Aspects of kinetics through elementary steps have been evaluated [14], with the system propionic acid and 1-propanol, obtaining the best model with a modified Eley–Rideal model. Moreover, the kinetics of butyric acid with butyl alcohol esterification were fitted to Eley–Rideal models [28]. SBA-15 immobilized *Candida antarctica* lipase B was used in the esterification of LA with isoamyl alcohol, and its kinetics was fitted to enzyme behavior with inhibition due to isoamyl alcohol [29]. On the other hand, the kinetics of production of ethyl, propyl, and butyl levulinates with Keggin heteropolyacids showed a short time pseudo-first order fitting, and an increased amount of activation energy with alkyl chain [30]. Sulfonic acid functionalized polystyrene coated coal fly ash catalyst was tested as a catalyst in the production of butyl levulinate; kinetic analysis was based on under reaction conditions as a pseudo-first-order reaction, considering a two-step consecutive reaction [31]. The kinetics of ethyl levulinate in the presence of Amberlyst-15 as the solid catalyst was studied considering diffusional effects; the classic esterification reaction mechanism consisting of two steps, protonation of the carboxylic group and nucleophilic attack of alcohol [32]. Recently, we reported the Preyssler catalyst in a Microwave-Assisted synthesis of butyl levulinate, considering steps of pseudohomogeneous for microwave effect and Langmiur–Hinshelwood–Hougen and Watson (LHHW) for catalytic effect [33].

As discussed in [33], although the pseudohomogeneous reversible model fits kinetics data of the batch reactor assisted with microwave irradiation, which is a useful simplification, it is important to consider we are dealing with solid surfaces, and kinetic models derived from heterogeneous approaches should be evaluated. On the other hand, no kinetic studies are available for the synthesis of pentyl levulinate, especially in a batch reactor-assisted microwave system using a commercial resin as a catalyst. Therefore, this study aims to demonstrate the effectiveness of the commercial acidic exchange resin Dowex® 50WX8 in the production of pentyl levulinate. The kinetic study revealed a good fit to the pseudohomogeneous reversible model, with slightly improved accuracy when integrated with the LHHW mechanism. ModEst software was employed for calculations, offering the advantage of excellent statistical analysis for the fitted parameters.

Materials and methods

Reagents

Commercial reagents were employed in the experiments without further processing. The reagents for the catalytic tests included levulinic acid (natural, 99 wt%,

Sigma-Aldrich), ethanol (anhydrous, HPLC grade, Soria), *n*-butanol (> 99 wt%, Sigma-Aldrich), isobutanol (99.5 wt%, Sigma-Aldrich), 2-butanol (99 wt%, Sigma-Aldrich), *n*-pentanol (99 wt%, Dorwil), and hexanol (98 wt%, Sigma-Aldrich). Strongly acidic exchange resin beads, Dowex® 50WX8 (hydrogen form, 50 to 100 mesh, Sigma-Aldrich) were used as a heterogeneous catalyst. The resin contains a cross-linkage of 8%, humidity ranging from 50 to 58%, a styrene–divinylbenzene (gel) matrix, and sulfonic acid as the active functional group [34, 35].

Esterification reaction

The esterification reaction involving levulinic acid and *n*-pentanol was conducted using a microwave-assisted batch reactor, employing a Monowave 400 instrument (Anton Paar) equipped with a type G4 borosilicate glass vial capped with silicone. The reactor had an operating volume between 0.5 and 2.0 mL, with a stirring speed of 600 rpm. In a standard experiment, the power peaked at 66 W (Fig. S1), 3 s after initiation, maintaining a stable level of around 3 W throughout the process. Various parameters were investigated, including the catalyst amount (5 to 30 mg), temperature (80 to 140 °C), *n*-pentanol: levulinic acid molar ratio (3:1 to 20:1), and the role of the solvent.

Identification of reaction products was performed using gas chromatography coupled with mass spectrometry (GC–MS) on a Shimadzu GCMQP2010 ultra, equipped with a Shimadzu AOC-20i injector and Agilent DB-1. Levulinic acid conversion and levulinate selectivity (ca. 100%) were assessed via gas chromatography using a Shimadzu 2014 with an SPB-1 column (30 m × 0.25 mm × 0.25 μm), FID detector, and employing the internal standard quantification method (octane 0.5 M).

The levulinic acid conversion (X_{LA}) and the initial reaction rate ($-r_0$) were calculated using Eqs. 1 and 2.

$$X_{LA}(\%) = \frac{n_{LA,0} - n_{LA,t}}{n_{LA,0}} \tag{1}$$

$$-r_0 = \frac{C_{LA,0} * V_0 * X}{\Delta t * m_{cat}} \tag{2}$$

Here $n_{LA,0}$ represents the initial moles of levulinic acid, $n_{LA,t}$ are the moles of levulinic acid at time t, $C_{LA,0}$ corresponds to the initial molar concentration of levulinic acid, V_0 is the total liquid volume, X is the levulinic acid conversion, Δt is the time interval (5 min), and m_{cat} is the catalyst mass.

Kinetic modeling

The levulinic acid esterification with *n*-pentanol produced pentyl levulinate, also known as amyl levulinate, depicted in Scheme 1. The experimental reaction conditions used are presented in Table 1, considering nine reaction times in the range of 0–90 min.
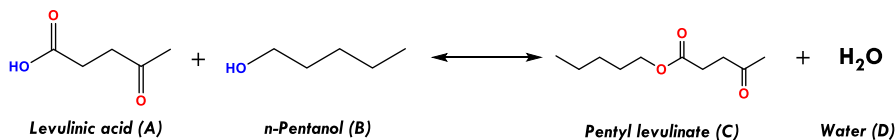
Scheme 1 Esterification reaction of levulinic acid with *n*-pentanol

Table 1 Experimental conditions for the levulinic acid esterification with *n*-pentanol over 50WX8 as a catalyst

Entry	Temperature (° C)	Mass of catalyst (mg)	*n*-Pentanol (mmol)
1	100	10	5
2	100	5	5
3	100	20	5
4	100	30	5
5	80	10	5
6	120	10	5
7	140	10	5
8	100	10	10
9	100	10	20
10	100	10	3

1 mmol of levulinic acid for all tests

Mass transfer limitations

Catalytic tests were performed under vigorous agitation (600 rpm) to overcome external mass-transfer limitations [36, 37]. Although small catalyst particles (<100 μm) were used to suppress the internal mass transfer limitations, the Weisz–Prater criterion (WP), given by Eq. 3, was used to evaluate if the reaction is limited or not by internal diffusion. If WP $\ll$ 1, the internal diffusion is negligible but if WP $\gg$ 1, internal diffusion limits the reaction [27, 37].

$$WP = \frac{-r_i^{exp} \rho_{cat} r_{cat}^2}{D_{i,\,eff} C_{i,\,cat}} \tag{3}$$

Here $-r_i^{exp}$ (mmol g^{-1} min^{-1}) is the reaction rate of specie i calculated from the experimental data, r_{cat} is the average radius of the catalyst particle (37.5 μm), ρ_{cat} is the catalyst density (1.04 g cm^{-3}), $C_{i,\,cat}$ is the concentration of specie i at the catalyst surface which can be assumed as the bulk concentration (C_i) when the absence of external mass transfer limitations is guaranteed, and $D_{i,\,eff}$ is the effective diffusivity of specie i through the catalyst, which is calculated as $D_{i,eff} = \varphi_p \sigma_c D_{i,L}/\tau$ where φ_p is the catalyst porosity (0.57, estimated in [38]), σ_c is the constriction factor (0.8 [37]), τ is the tortuosity (3.0 [37]), and $D_{i,L}$ is the diffusion coefficient of specie i in 1-pentanol at the specific temperature. It is noteworthy that the criterion gives an upper bound to avoid internal mass transfer limitations, which indicates that is enough to use the maximum value of $-r_i^{exp}$, corresponding to $-r_{i0}^{exp}$ (Eq. 2).

Table 2 Heterogeneous kinetic models proposed based on Langmuir–Hinshelwood–Hougen–Watson (LHHW) and Eley–Rideal (ER) approaches

Model	Reaction rate (r)	Description
ER1	$\dfrac{k\left[K_A C_A C_B - \frac{C_C C_D}{K_S K_C}\right]}{\left[1 + K_A C_A + \frac{C_C}{K_C}\right]}$	Eley–Rideal model, surface reaction as the rate-limiting step ($k = k_S C_t$), levulinic acid is adsorbed, pentyl levulinate is desorbed
ER2	$\dfrac{k\left[\frac{K_S K_B C_A C_B}{C_D} - \frac{C_C}{K_C}\right]}{\left[1 + K_B C_B + \frac{K_S K_B C_A C_B}{C_D}\right]}$	Eley–Rideal model, desorption as the rate-limiting step ($k = k_C C_t$), pentanol is adsorbed, pentyl levulinate is desorbed
LH1	$\dfrac{k\left[K_A K_B C_A C_B - \frac{C_C C_D}{K_S K_C K_D}\right]}{\left[1 + K_A C_A + K_B C_B + \frac{C_C}{K_C} + \frac{C_D}{K_D}\right]^2}$	LHHW model, surface reaction as the rate-limiting step ($k = k_S C_t^2$), both reactants are adsorbed, both products are desorbed

k and K_i denote the reaction rate and the equilibrium constants

Pseudo-homogeneous kinetic model

A pseudo-homogeneous reversible model was proposed based on previous studies for levulinic acid esterification in microwave-assisted batch reactors [39, 40]. This approach serves as an acceptable initial step in the kinetic modeling, albeit with several underlying assumptions [41–43]. It assumes a homogeneous distribution of reactive species on the catalyst surface and overlooks the catalysts' structural intricacies. Additionally, due to its high level of simplification, the model may heavily rely on adjusted parameters and might lack generalizability to diverse experimental conditions.

The mole balance for the species in the liquid phase in the batch reactor is represented by Eq. 4, where C_i is the concentration of species i, m_{cat} is the catalyst mass, V_R is the reaction volume, ν is the stoichiometric coefficient (-1 for reactants and $+1$ for products), t is the reaction time, and r is the generation rate, given by Eq. 5. The reaction rate constants (k_1 and k_2 for forward and reverse directions, respectively) are calculated through the modified Arrhenius equation, Eq. 6, where k_{ref} denotes to the reaction constant at an average temperature ($T_{ref} = 100$ °C), Ea is the activation energy, T is the absolute temperature, and R is the gas constant. α, β, γ, and δ represent the reaction orders for levulinic acid, pentanol, pentyl levulinate, and water. Equation 6 is preferably employed to enhance the statistical estimation of temperature-dependent parameters by incorporating a reference constant (k_{ref}) [36, 44]. This is particularly beneficial because the experiments are centralized, suppressing the correlation between the parameters. Moreover, proposing an initial guess for k_{ref} is notably simpler than determining the frequency factor in nonlinear regression.

$$\frac{dC_i}{dt} = \frac{m_{cat}}{V_R}\nu r \quad (i = A, B, C, D) \tag{4}$$

$$r = k_1 C_A^\alpha C_B^\beta - k_2 C_C^\gamma C_D^\delta \tag{5}$$

$$k = k_{ref}e^{-\frac{E_a}{R}\left(\frac{1}{T} - \frac{1}{T_{ref}}\right)} \tag{6}$$

Heterogeneous models

In our recent work [33], we considered both the microwave effect ($r_{MW} = r$, Eq. 5) and the catalytic effect (r_{Cat}) as synergistic contributions in the kinetic modeling of the esterification of levulinic acid over a Preyssler catalyst. The design equation for the reactor is established by Eq. 7, where r_{Het} corresponds to the reaction rate laws of different heterogeneous models given in Table 2. The proposed models draw inspiration from the best heterogeneous models reported previously for the esterification of lauric acid [45], trans-cinnamic acid [46], and levulinic acid [33], and the derivation of these expressions can be found in the Supporting Information. It is worth mentioning that the microwave term in Eq. 7 is independent of the catalyst mass, differing from the pseudo-homogeneous model. Table 2 illustrates two models deduced from the Eley–Rideal (ER) approach, which assumes that only one reactant is adsorbed on the catalyst surface. Additionally, one model was deduced from the Langmuir–Hinshelwood–Hougen–Watson (LHHW) approach, assuming the adsorption of both reactants.

$$\frac{dC_i}{dt} = \nu(r_{MW} + r_{Cat}) = \nu\left(r_{MW} + \frac{m_{cat}}{V_R}r_{Het}\right) (i = A, B, C, D) \tag{7}$$

Parameters optimization

The parameter estimation was performed with the software ModEst [47] using the squared difference between the experimental and calculated concentrations, as defined by Eq. 8. The difference (S.E) was minimized by using the Levenberg–Marquardt algorithm and the determination coefficient (R^2), Eq. 9 served as a suitable metric for assessing the goodness of fit, which compares the model performance to the variance of all experimental points. The statistical reliability of the parameters was evaluated using the Markov Chain Monte Carlo (MCMC) analysis [44, 48], which models the uncertainties in the data as statistical distributions. $C_{j,i, Exp}$ and $C_{j,i, Mod}$ refer to the experimental and modeled concentrations of the specie j for each run i, while $\overline{C}_{j,i, Exp}$ refers to the mean of the experimental concentrations data.

$$S.E = \sum_{j}^{N_{com}} \sum_{i=1}^{N_{obs}} \left(C_{j,i, Exp} - C_{j,i, Mod}\right)^2 \tag{8}$$

$$R^2(\%) = 100\left(1 - \frac{\sum_{j}^{N_{com}} \sum_{i=1}^{N_{obs}} \left(C_{j,i, Exp} - C_{j,i, Mod}\right)^2}{\sum_{j}^{N_{com}} \sum_{i=1}^{N_{obs}} \left(C_{j,i, Exp} - \overline{C}_{j,i, Exp}\right)^2}\right) \tag{9}$$

Results and discussion

Effect of the reaction conditions

The microwave effect has been previously studied, utilizing various catalysts for the esterification of levulinic acid, such as SAPO-34 [49], recyclable sulfated amorphous nanosilica [50], and a Preyssler-type heteropolyacid on silica [33]. The positive effect is clearly reflected in the increased reaction rate of levulinic acid when assisted by microwaves, as reported in the esterification of levulinic acid with *n*-butanol [33]. Increases in conversion of ca. 30%, 28%, 17%, and 14% (difference in conversion with and without catalyst) after 180 min were obtained for the reaction carried out at 100, 120, 140, and 160 °C. Therefore, in this study, a strongly acidic exchange resin like Dowex® 50WX8 was demonstrated as a highly active catalyst for the esterification of levulinic acid, surpassing the effectiveness of a previous report from our group based on a Preyssler heteropolyacid supported on silica (PCSiO$_2$) [33], as illustrated in Fig. 1. The initial reaction rates for the esterification were calculated at different temperatures, revealing significantly high values of 3.42, 4.62, and 8.02 mmol g^{-1} min^{-1} over 5WX8 at 100, 120, and 140 °C. These values are much higher than the corresponding rates over PCSiO$_2$, such as 0.18, 0.30 and 0.63 mmol g^{-1} min^{-1}. At 100 °C, the reaction rate with 50WX8 is approximately 20 times higher than the reaction rate with PCSiO$_2$.

The effect of temperature on the esterification of levulinic acid was investigated at four temperatures (80, 100, 120, and 140 °C), as illustrated in Fig. 2A. The conversion profiles exhibit the expected shape, indicating an increase in catalytic activity (reflected in the conversion) with temperature, as predicted by the Arrhenius equation. Conversions of ca. 33%, 61%, 93% and 96% were achieved at 80, 100, 120 and 140 °C after 90 min. These values can be considered as the equilibrium conversions at those temperatures, as the levulinic acid conversion remains almost constant after 60 min. On the other hand, Fig. 2B displays the plot of the initial reaction rate as a function of the inverse of temperature, which is used to estimate the activation energy of the formation of pentyl levulinate. A suitable linear trend is observed in Fig. 2B, resulting in Ea = 44.6 kJ mol^{-1}. This value could be validated with the optimized parameters in the kinetic modeling using the different proposed models.

The effect of the amount of 50WX8 on the esterification reaction was evaluated using 5, 10, 20, and 30 mg at 100 °C, as shown in Fig. 3A. Clearly, levulinic acid conversion is directly proportional to the catalyst amount, resulting in conversions of ca. 49%, 61%, 71%, and 81% after 90 min. This behavior can be easily explained by the increase in the number of active acid sites available for the catalytic reaction. Furthermore, Fig. 3B confirms that the esterification reaction follows a catalytic route, as evidenced by the observed dependence between the initial reaction rate and the catalyst mass. The variation in this parameter is crucial for the kinetic modeling of the esterification reaction, as will be demonstrated later.

The investigation into the excess of pentanol in the esterification reaction with levulinic acid was conducted using four molar ratios of alcohol to levulinic acid: 3:1, 5:1, 10:1 and 20:1, at 100 °C with 10 mg of catalyst. Fig. 4 illustrates that catalytic

activity, as reflected in the conversion, improved at lower molar ratios, resulting in values of ca. 61%, 60%, 50%, and 45% after 90 min. A similar trend was observed when *n*-butanol was used as the alcohol, and PCSiO$_2$ and magnetic materials based on Keggin heteropolyacids were employed as heterogeneous catalysts [33, 51]. In contrast, no dependence of the conversion on the molar ratios of ethanol to lauric acid, ranging between 10.7 and 64.2, was observed when using a Keggin-heteropolyacid on silica as a catalyst [45]. The low conversion at high ratios can be explained by the high dilution of levulinic acid and potential mass transfer limitations due to difficulties in levulinate diffusion in the medium. This could result in high local concentrations, limiting the overall efficiency of the esterification reaction [52, 53]. This parameter will be considered later in the kinetic modeling.

Role of the alcohol

Various alcohols were tested in the esterification reaction with levulinic acid at 100 °C, employing 10 mg of catalyst and alcohol: levulinic acid molar ratio of 5:1. Fig. 5A demonstrates levulinic acid conversions exceeding 55% for most solvents after 90 min, except for 2-butanol, which yielded only 21%. Fig. 5B aimed to establish a relationship between the conversion and the dielectric constant of the alcohols [54, 55]; however, no defined trend was observed. In general terms, primary alcohols (ethanol, *n*-butanol, *n*-pentanol, and 1-hexanol) facilitated high
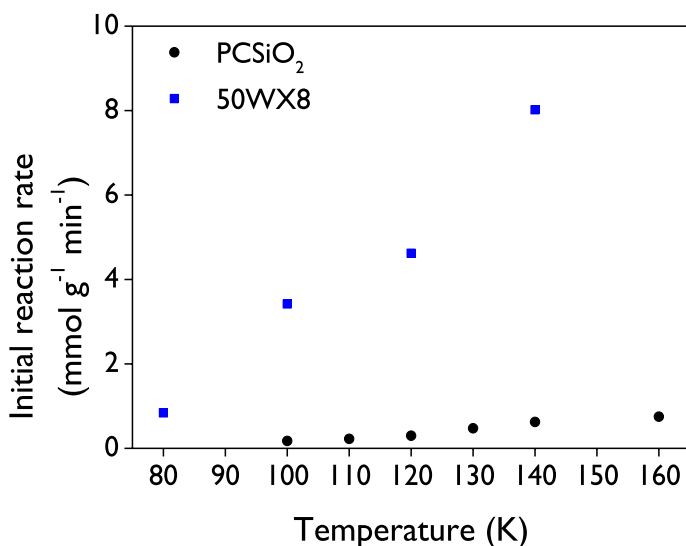

Fig. 1 Initial reaction rates for the levulinic acid esterification in a microwave-assisted reactor as a function of the temperature over two heterogeneous catalysts: 50WX8 (this study) and PCSiO$_2$ (a Preyssler-type heteropolyacid supported on silica [33]). Reaction conditions: 1 mmol of levulinic acid, 5 mmol of *n*-butanol
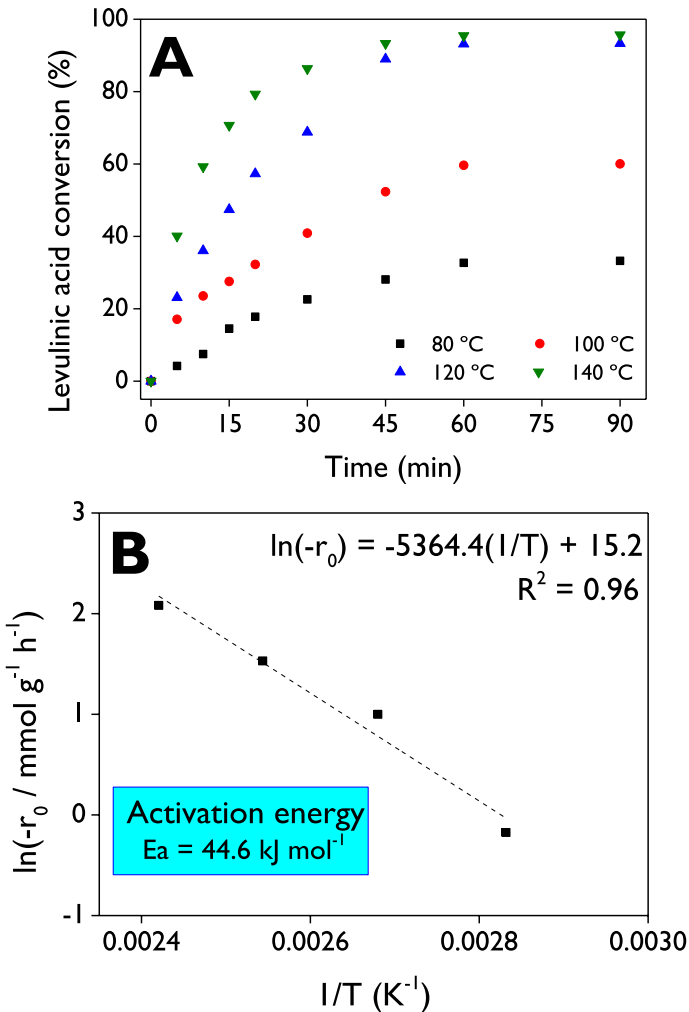
Fig. 2 **A** Levulinic acid conversion as a function of time for different temperatures. **B** Estimation of the activation energy. Reaction conditions: 1 mmol of levulinic acid, 5 mmol of pentanol, 10 mg of 50WX8 as a catalyst

levulinic acid conversions, ranging between 61 and 72%. When evaluating some isomers of $C_4H_{10}O$, such as *n*-butanol, isobutanol, and 2-butanol, appreciable differences in their activity were observed. Although both *n*-butanol and isobutanol are primary alcohols with similar polarity, as reflected in the dielectric constant, they resulted in significantly different conversions of ca. 70% and 55% after 90 min. This difference can be attributed to the linear structure of *n*-butanol, while the branched structure of isobutanol introduces steric hindrance, affecting the efficiency of the esterification reaction. Similarly, with a secondary alcohol like 2-butanol, a levulinic acid conversion of ca. 21% was achieved. This low
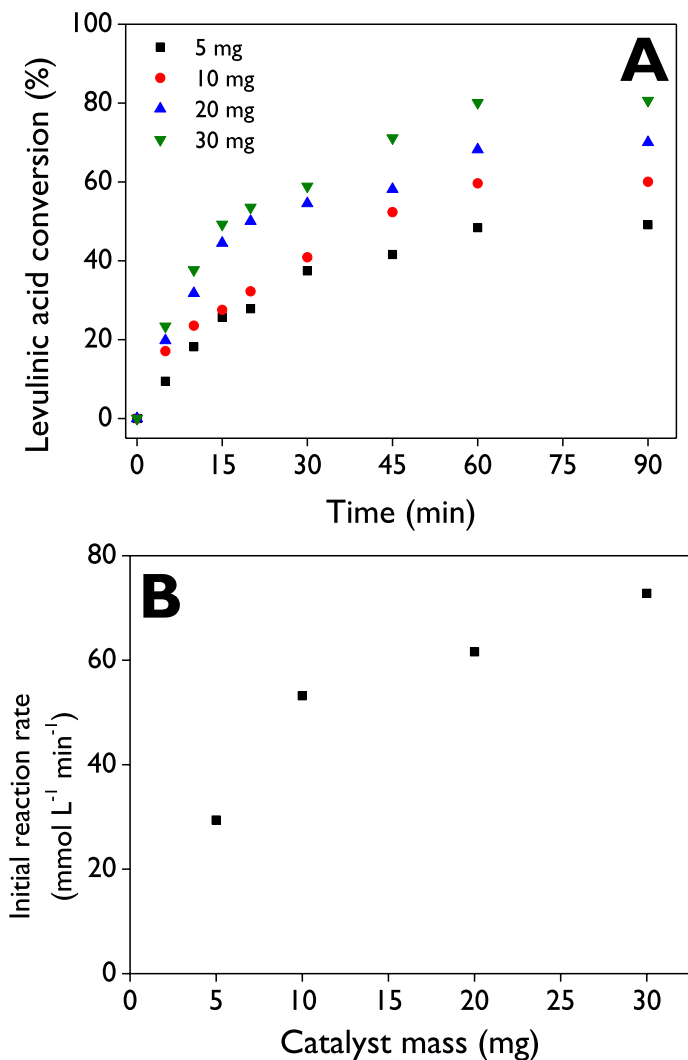
Fig. 3 **A** Levulinic acid conversion as a function of time for different amounts of catalyst. **B** Initial reaction rate of levulinic acid as function of the catalyst mass. Reaction conditions: 1 mmol of levulinic acid, 5 mmol of pentanol, 100 °C, 50WX8 as a catalyst

value can be explained by the higher steric effect on the secondary carbon compared to primary alcohols. Similar conclusions were drawn in a previous study on the esterification reaction of stearic acid with 1-butanol and 2-butanol using a montmorillonite-based clay catalyst [56]. Additionally, in the esterification of lauric acid with *n*-butanol, *s*-butanol, and *tert*-butanol, using a Keggin heteropolyacid on silica, comparable findings were observed [45]. The importance of the role of alcohol in the esterification reaction has been investigated using the Taft
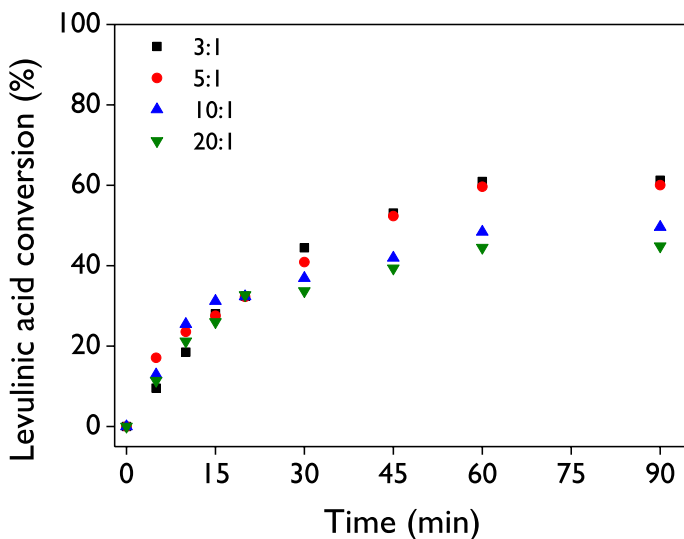
Fig. 4 Levulinic acid conversion as a function of time for different pentanol/acid molar ratios. Reaction conditions: 1 mmol of levulinic acid, 10 mg of 50WX8 as a catalyst, 100 °C

concept [57] in the esterification of propanoic acid, which concludes the importance of steric hindrance in the reactivity of the alcohol.

Robustness of acidic resin as a catalyst

The robustness of the Dowex® 50WX8 catalyst was investigated through two cycles of reusability, as illustrated in Fig. 6. The profiles of levulinic acid conversion demonstrated that catalytic activity can be completely recovered after two reuses of the commercial acidic resin. Conversions ranging between 60 and 64% after 90 min at 100 °C with 10 mg of catalyst are obtained in both the fresh and reused cycles. These results highlight the high catalyst stability of this material compared to some heteropolyacids previously reported for levulinic acid esterification [5, 33]. Surprisingly, there are reports with heteropolyacids where it is stated that there is no loss of activity after more than three or four reuses [51, 58, 59].

Furthermore, these reusability results indicate the significant advantages of the commercial catalyst used in this contribution because it does not require complex synthesis procedures, as is the case with supported heteropolyacids. The latter demand intensive energy use and the use of substances such as phosphoric acid and ethanol [33], or the use of not very reproducible methodologies for anchoring into supports, such as incipient wetness impregnation [5]. On the other hand, the use of commercial catalysts guarantees reproducibility in the efficiency of the reaction and is easily available in the market. These aspects are extremely important for scaling-up chemical processes [60].
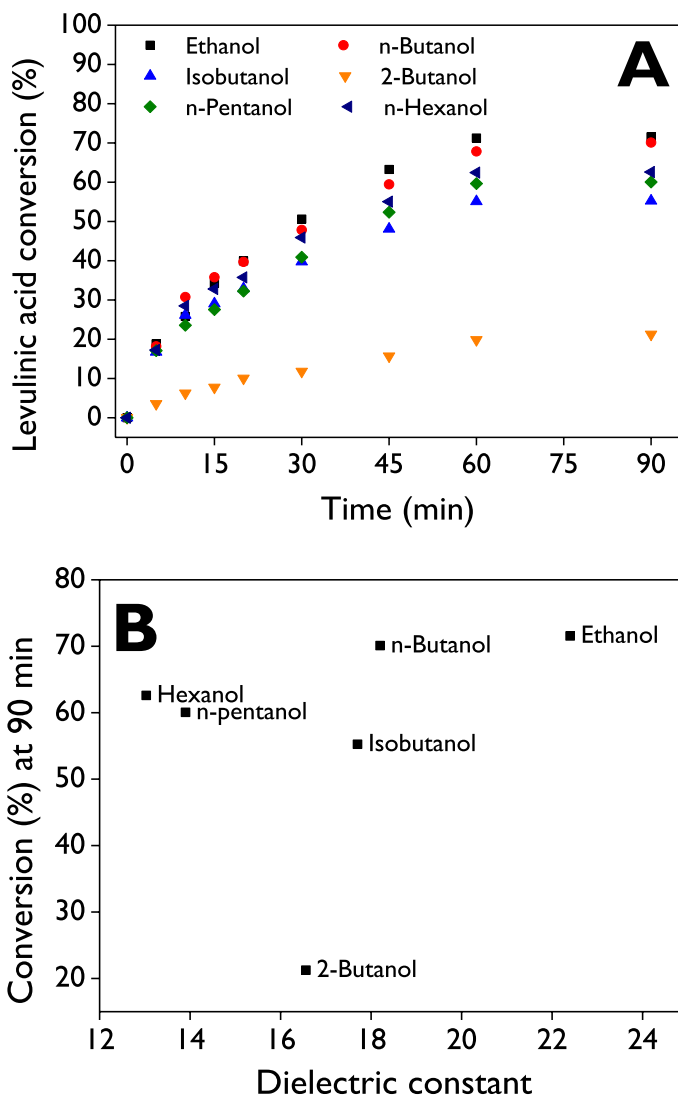
Fig. 5 **A** Effect of the alcohol nature on the levulinic acid esterification. **B** Levulinic acid conversion as a function of the dielectric constant. Reaction conditions: 1 mmol of levulinic acid, 5 mmol of alcohol, 10 mg of 50WX8 as a catalyst, 100 °C

Kinetic modeling

Internal mass transfer limitations

Table 3 presents the Weisz–Prater criterion (WP) results for levulinic acid, demonstrating satisfaction across all experimental runs. It is noted that internal mass transfer limitations are absent, indicating no discernible concentration gradients within

the catalyst. Thus, it is inferred that the esterification of levulinic acid with 1-pentanol over 50WX8 is under kinetic control.

Pseudo-homogeneous model

The pseudo-homogeneous reversible kinetic model, based on power law expressions, proves to be a suitable expression for describing both the microwave and catalytic effect on the esterification of levulinic acid with pentanol. The determination coefficient ($R^2 = 99.88\%$, Table 4) adequately accounts for the variability in the experimental concentration data of all species, offering a highly simplified yet effective kinetic model.

This numeral fitting surpasses the performance of a comparable model in a previous study involving a microwave-assisted reactor for levulinic acid with n-butanol over $PCSiO_2$, yielding an R^2 value of 94.97% [33]. In contrast, earlier studies without microwaves, focusing on the esterification of lauric acid [45] and trans-cinnamic acid [46], demonstrated poor fittings with R^2 values of 85.79% and 69.47%, respectively.

Table 4 reports the optimized kinetic parameters, revealing activation energies of 59.5 and 26.9 kJ mol^{-1} for the forward and reverse directions in the esterification route outlined in Scheme 1. Notably, these values differ significantly from the corresponding ones reported previously when $PCSiO_2$ was used as a catalyst, with values of 42.4 and 40.3 kJ mol^{-1} [33]. However, the activation energy for the forward reaction aligns with the values obtained in similar contexts, such as with methanesulfonic acid and hexanol ($E_a = 61$ kJ mol^{-1}) [63] and with desilicated zeolite β and
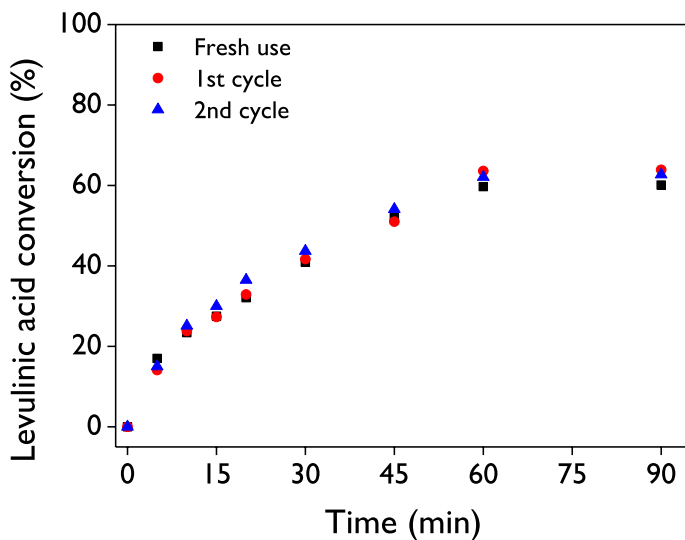

Fig. 6 Reusability test of Dowex® 50WX8 as the catalyst on the levulinic acid esterification. Reaction conditions: 1 mmol of levulinic acid, 5 mmol of pentanol, 10 mg of catalyst, 100 °C. The catalyst was recovered by filtration and dried under vacuum conditions at room temperature

1,2-ethanediol ($E_a = 53.0$ kJ mol^{-1}) [64]. More detailed information can be found in Table 6 of our previous report [33]. Table 4 presents the reaction rate constants for both reactions at 100 °C. Consequently, the pre-exponential factor for each direction can be determined using the Arrhenius equation.

The overall reaction orders are 10.27 and 11.47 for the forward and reverse reactions. It is noteworthy that while the corresponding value for the reverse reaction remains constant, the reaction orders concerning ester and water are interdependent. This is because $11.47 = \gamma + \delta$, given that molar concentrations of ester and water are equal at any time ($C_C = C_D$), due to the stoichiometric factor being 1:1 and the absence of these products at the beginning of the reaction. Furthermore, the results suggest a higher dependence of the reaction rate on pentanol concentration compared to the concentrations of levulinic acid and the products, as reflected in its elevated reaction order ($\beta = 8.5$). The dependence observed could be attributed to the high concentration of pentanol in the reaction medium, which directly influences the reaction rate due to the availability of pentanol molecules. Additionally, the interactions of the alcohol with the catalyst could be more sensitive, further impacting the reaction rate. In contrast, when PCSiO$_2$ was used as a catalyst [33], a higher dependence of the reaction rate was observed with the concentration of levulinic acid, rather than the alcohol (*n*-butanol).

The comparison between the experimental concentration profiles and those calculated with the pseudo-homogeneous reversible kinetic model is illustrated in Fig. S2. The results demonstrate that kinetics based on homogeneity can effectively capture the behavior of the molar concentrations for the four species during the studied time interval. The statistical reliability of the kinetic parameters was evaluated using MCMC analysis. Fig. S6 shows plots of the probability density contour for the correlation of pairs of parameters, with a total of 28 combinations. Strong correlations are suggested for the pairs k_1 and k_2, as well as the pairs resulting from combinations

Table 3 Weisz–Prater criterion for the 10 experiments

Entry	m_{cat} (mg)	V (mL)	T (K)	C_0 (mol L^{-1})	$-r_0$ (mmol g^{-1} min^{-1})	μ_B (cP)	D_{AB} (cm^2 s^{-1})	D_{eff} (cm^2 s^{-1})	WP
1	10	0.643	373	1.56	3.42	0.644	2.24E−05	3.40E−06	0.157
2	5	0.643	373	1.56	3.78	0.644	2.24E−05	3.40E−06	0.174
3	20	0.643	373	1.56	1.98	0.644	2.24E−05	3.40E−06	0.091
4	30	0.643	373	1.56	1.56	0.644	2.24E−05	3.40E−06	0.072
5	10	0.643	353	1.56	0.84	0.929	1.47E−05	2.23E−06	0.059
6	10	0.643	393	1.56	4.62	0.465	3.27E−05	4.97E−06	0.146
7	10	0.643	413	1.56	8.02	0.347	4.61E−05	7.01E−06	0.179
8	10	1.184	373	0.84	2.58	0.644	2.24E−05	3.40E−06	0.219
9	10	2.266	373	0.44	2.28	0.644	2.24E−05	3.40E−06	0.370
10	10	0.427	373	2.34	1.91	0.644	2.24E−05	3.40E−06	0.058

$-r_0$ was calculated with Eq. 2. μ_B was calculated from reference [61]. The diffusion coefficient of levulinic acid in 1-pentanol (D_{AB}) was calculated using the Wilke–Chang equation [62], using 1.0 for the association parameter of 1-pentanol and 123.196 cm^3 mol^{-1} for the molar volume of the levulinic acid at the normal boiling point

Table 4 Kinetic parameters for the pseudo-homogeneous reversible model

Parameter	Units	Value	Standard error (%)
k_1	$mol^{-9.27}\ L^{10.27}\ g^{-1}\ min^{-1}$	5.22×10^{-11}	91.4
k_2	$mol^{-10.47}\ L^{11.47}\ g^{-1}\ min^{-1}$	1.95×10^{-12}	>100
Ea_1	$kJ\ mol^{-1}$	59.5	3.7
Ea_2	$kJ\ mol^{-1}$	26.9	>100
α	–	1.77	5.0
β	–	8.5	5.4
γ	–	6.55	>100
δ	–	4.92	>100
R^2	%	99.88	–

k_1 and k_2 values were estimated at 100 °C

of the two activation energies with the four reaction orders due to their elongated shapes [44, 65]. It is coherent, for instance, for γ and δ, as mentioned above. It is noteworthy that the high density of contour lines in the plots of all parameters with k_1 and k_2 (those that do not show strong correlations) represents regions where the joint probability is higher, indicating more constrained or well-defined parameter values. In contrast, plots exhibiting low density suggest areas of lower joint probability, indicating higher uncertainty or less constraint on parameter values.

The marginal distributions from the MCMC analysis (Fig. S7) for the individual parameters along the axes depict the probability distribution of each parameter independently [65]. Distributions for k_1, k_2, and Ea_1 are approximately Gaussian, suggesting that these model parameters are well-constrained. In contrast, Fig. S7 shows that the distribution for Ea_2 exhibited a very poor maximum, reflected in its high standard error (Table 4) [44]. The distribution for α presents a bimodal-like shape with maxima at 1.771 and 1.768, with the former being the most probable value for that parameter, as reported in Table 4.

Heterogeneous models

In this case, the microwave effect on the esterification reaction was modeled using the pseudo-homogeneous reversible model, and the catalytic effect was modeled using three heterogeneous kinetic models, as previously mentioned in Eq. 7. This strategy was successfully demonstrated in our recent work [33]. Although a very high fitting was achieved with only the pseudo-homogeneous model, as discussed above, it is pertinent to adjust the experimental data to a more realistic phenomenology in the system, considering the presence of a heterogeneous catalyst.

Therefore, Table 5 reports the kinetic parameters for the set of models, which include the pseudo-homogeneous and three heterogeneous models (ER1, ER2, and LH1). Results demonstrate slightly better numerical fittings of these three models than the pseudo-homogeneous one, with determination coefficients greater than 99.94%. However, it is possible to discern between the models by first considering the values of activation energies of the catalytic part, i.e. Ea = 58.4, 60.2, and

50.6 kJ mol^{-1} for ER1, ER2, and LH1. Notice that the value for LH1 is the closest to the estimated value (Ea = 44.6 kJ mol^{-1}) in Fig. 2B using the calculation of the initial reaction rates. On the other hand, the activation energy values for the reverse reaction in the pseudo-homogeneous part for the expressions derived from the Eley–Rideal approach exhibited very high values (Ea$_2$ = 105 kJ mol^{-1} for ER1) or very low values (Ea$_2$ = 1.0 kJ mol^{-1} for ER2), which are not expected values for this esterification route [33]. Furthermore, Fig. S3 shows the comparison between the experimental concentration profiles and those calculated with the LH1 model, demonstrating the success of the kinetic modeling. The numerical fitting for the ER1 and ER2 models is shown in Figs. S4 and S5.

The results with the LH1 model, like the pseudo-homogeneous model, suggest a higher dependence of the reaction rate on pentanol concentration compared to the concentrations of levulinic acid and the products, as reflected in the value of β = 6.51. The equilibrium constants for the LH1 model conclude about the adsorption strength over the 50WX8 catalyst, decreasing in the following order: pentyl levulinate (1/K$_C$ = 2.01 L mol^{-1}), pentanol (K$_B$ = 0.335 L mol^{-1}), water (1/K$_D$ = 5.26 × 10^{-3} L mol^{-1}), and levulinic acid (K$_A$ = 7.8 × 10^{-4} L mol^{-1}). The contour plots from the MCMC analysis for the LH1 model can be found in the Supporting Information (Sect. 4.2) for all the pairs of combinations (105 in total corresponding to the 15 kinetic parameters).

The marginal distributions in the form of histograms for the LH1 model from the MCMC analysis are shown in Fig. S8 for the 15 individual parameters. Distributions for k$_1$, k$_2$, Ea$_2$, α, δ, and K$_S$ have a Gaussian-like shape, indicating well-constrained values in the model. For other parameters, the distribution is not symmetrical, but in general terms, the most probable value observed as the maximum in each distribution corresponds to the value reported in Table 5.

Reaction pathway

A plausible reaction mechanism for the esterification of levulinic acid with *n*-pentanol (amyl alcohol) over Dowex® 50WX8 (DowexH, hydrogen form) is proposed in Scheme 2, considering the reported literature on the reaction of propionic acid with 1-propanol [14]. Five reaction stages can be proposed for the esterification reaction based on the best heterogeneous model obtained previously, such as LHHW, and consistent with the kinetic numeral fitting.

Firstly, levulinic acid is adsorbed on the Dowex® resin, and subsequently, this resin in an acidic form transfers a proton for the formation of the carbocation, which is subsequently captured by the non-bonding electron pairs of the carbonyl oxygen. Through a resonance phenomenon, a more stable carbocation is generated in this manner, thus activating the system **(I)**. Then, *n*-pentanol is adsorbed onto the surface catalyst **(II)**. In the third stage, the activated carbocation is attacked by *n*-pentanol, resulting in the formation of protonated pentyl levulinate and a water molecule, both adsorbed on the catalyst **(III)**. Finally, the protonated levulinate loses the proton and

Table 5 Kinetic parameters for the heterogeneous models coupled with the pseudo-homogeneous model

Parameter	Units	ER1		ER2*		LH1*	
		Value	S.E (%)	Value	S.E (%)	Value	S.E (%)
k_1	$(mol\ L^{-1})^{1-\alpha-\beta}\ min^{-1}$	2.84×10^{-11}	>100	4.72×10^{-3}	>100	1.42×10^{-8}	>100
k_2	$(mol\ L^{-1})^{1-\gamma-\delta}\ min^{-1}$	1.84×10^{-6}	>100	2.03×10^{-6}	>100	1.01×10^{-7}	>100
Ea_1	$kJ\ mol^{-1}$	72.8	9.3	71.7	13.7	72.5	13.4
Ea_2	$kJ\ mol^{-1}$	105	>100	1.0	>100	37.0	>100
α	–	2.71	7.9	1.45	18.7	1.79	11.3
β	–	9.67	14.5	9.98×10^{-5}	>100	6.51	24.7
γ	–	4.90	>100	9.97	>100	2.68	>100
δ	–	4.44	>100	10.0	>100	2.76	>100
k	$L\ g^{-1}\ min^{-1}$	9.55	>100	4.2×10^{-3}	22.8	6.57	0.0
Ea	$kJ\ mol^{-1}$	58.4	10.0	60.2	9.8	50.6	15.0
K_A	$L\ mol^{-1}$	7.74×10^{-6}	>100	–	–	7.8×10^{-4}	0.0
K_B	$L\ mol^{-1}$	–	–	7.44×10^{4}	>100	3.35×10^{-1}	0.0
K_C	$mol\ L^{-1}$	1.21×10^{4}	>100	9.36×10^{4}	>100	4.98×10^{-1}	>100
K_D	$mol\ L^{-1}$	–	–	–	–	1.90×10^{2}	>100
K_S	–	3.12×10^{4}	>100	8.28×10^{-2}	>100	1.12×10^{4}	>100
R^2	%	99.94	–	99.96	–	99.94	–

k, k_1, and k_2 values were estimated at 100 °C

*Units of the parameter k are $mol\ g^{-1}\ min^{-1}$

is desorbed of the catalyst **(IV)**, and the desorption of water occurs **(V)**, thereby regenerating the catalyst.

Conclusions

Dowex® 50WX8 emerged as a highly active and selective commercial catalyst for the esterification of levulinic acid with pentanol under microwave irradiation, yielding levulinate, a potent compound with noteworthy applications as an oxygenated additive to biofuels, facilitating a substantial reduction in pollutant emissions. The systematic exploration of critical parameters, including the pentanol/acid molar ratio, reaction temperature, and catalyst amount, provided valuable insights into the kinetic behavior of the reaction. The integration of a dual-model approach, combining a pseudo-homogeneous model to address the microwave effect and catalytic contributions modeled through LHHW and Eley–Rideal mechanisms, yielded a comprehensive understanding of the reaction kinetics.

The selection of the most fitting model, guided by Markov Chain Monte Carlo (MCMC) analysis derived from contour plots depicting the relationship between pairs and MCMC distributions, revealed that the LHHW model with the surface reaction as the limiting step effectively captured the complexities of the esterification process. The determined activation energy of 50.6 kJ mol^{-1} provides critical
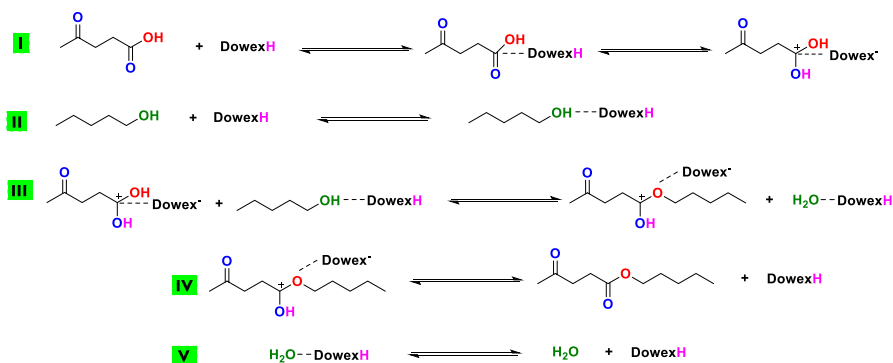
Scheme 2 Plausible reaction mechanism for the esterification of levulinic acid over Dowex® 50WX8 as a catalyst

insights into the catalytic synthesis of pentyl levulinate, underscoring the significance of Dowex® 50WX8 in this reaction.

This study further elucidated the crucial role of alcohol in the esterification route, explaining its influence on the reaction pathway and confirming the detrimental influence of alcohol structures with higher steric hindrance. The confirmed catalytic stability of the commercial catalyst over multiple cycles underscores its practical applicability. Notably, the absence of mass transfer limitations, as demonstrated by the Weisz–Prater criterion, enhances confidence in the reliability of our findings and the developed kinetic modeling.

In summary, this research not only advances our comprehension of the kinetic aspects of levulinic acid esterification but also establishes a robust foundation for future studies. The proposed reaction pathway and insights gained contribute valuable knowledge to the field, emphasizing the promising role of Dowex® 50WX8 as a catalyst in the synthesis of pentyl levulinate.

References

1. Nelson Appaturi J, Andas J, Ma YK et al (2022) Recent advances in heterogeneous catalysts for the synthesis of alkyl levulinate biofuel additives from renewable levulinic acid: a comprehensive review. Fuel 323:124362. https://doi.org/10.1016/j.fuel.2022.124362

2. Badgujar KC, Bhanage BM (2015) Thermo-chemical energy assessment for production of energy-rich fuel additive compounds by using levulinic acid and immobilized lipase. Fuel Process Technol 138:139–146. https://doi.org/10.1016/j.fuproc.2015.05.015

3. Castro GAD, Fernandes SA (2021) Microwave-assisted green synthesis of levulinate esters as biofuel precursors using calix[4]arene as an organocatalyst under solvent-free conditions. Sustain Energy Fuels 5:108–111. https://doi.org/10.1039/d0se01257b

4. Trombettoni V, Sciosci D, Bracciale MP et al (2018) Boosting biomass valorisation. Synergistic design of continuous flow reactors and water-tolerant polystyrene acid catalysts for a non-stop production of esters. Green Chem 20:3222–3231. https://doi.org/10.1039/c8gc00824h

5. Pithadia D, Patel A, Hatiya V (2022) 12-Tungstophosphoric acid anchored to MCM-22, as a novel sustainable catalyst for the synthesis of potential biodiesel blend, levulinate ester. Renew Energy 187:933–943. https://doi.org/10.1016/j.renene.2022.01.106

6. Palma V, Barba D, Cortese M et al (2020) Microwaves and heterogeneous catalysis: a review on selected catalytic processes. Catalysts 10:246. https://doi.org/10.3390/catal10020246

7. Szabó Y, Kiss MA, Kónya Z et al (2023) Microwave-induced base-catalyzed synthesis of methyl levulinate, a further improvement in dimethyl carbonate-mediated valorization of levulinic acid. Appl Catal A. https://doi.org/10.1016/j.apcata.2022.119020

8. Silva Junior MM, Portugal LA, Serra AM et al (2017) On line automated system for the determination of Sb(V), Sb(III), thrimethyl antimony(v) and total antimony in soil employing multisyringe flow injection analysis coupled to HG-AFS. Talanta 165:502–507. https://doi.org/10.1016/j.talanta.2016.12.022

9. Duff MC, Amrhein C (1996) Method for the separation of uranium(IV) and (VI) oxidation states in natural waters. J Chromatogr A 743:335–340. https://doi.org/10.1016/0021-9673(96)00235-X

10. Nedjadi Y, Bailat C, Caffari Y et al (2012) A new measurement of the half-life of ^{166m}Ho. Appl Radiat Isot 70:1990–1996. https://doi.org/10.1016/j.apradiso.2012.02.063

11. Cervantes A, Rodríguez R, Ferrer L et al (2017) Automatic solid phase extraction of cadmium exploiting a multicommutated flow system previous ICP-MS detection: application to tobacco samples. Microchem J 132:107–111. https://doi.org/10.1016/j.microc.2017.01.016

12. Monazam E, Siriwardane R, Miller D, McIntyre D (2018) Rate analysis of sorption of Ce^{3+}, Sm^{3+}, and Yb^{3+} ions from aqueous solution using Dowex 50W-X8 as a sorbent in a continuous flow reactor. J Rare Earths 36:648–655. https://doi.org/10.1016/j.jre.2017.10.010

13. Miller DD, Siriwardane R, Mcintyre D (2018) Anion structural effects on interaction of rare earth element ions with Dowex 50W X8 cation exchange resin. J Rare Earths 36:879–890. https://doi.org/10.1016/j.jre.2018.03.006

14. Ali SH, Tarakmah A, Merchant SQ, Al-Sahhaf T (2007) Synthesis of esters: development of the rate expression for the Dowex 50 Wx8-400 catalyzed esterification of propionic acid with 1-propanol. Chem Eng Sci 62:3197–3217. https://doi.org/10.1016/j.ces.2007.03.017

15. Korkmaz S, Salt Y, Hasanoglu A et al (2009) Pervaporation membrane reactor study for the esterification of acetic acid and isobutanol using polydimethylsiloxane membrane. Appl Catal A 366:102–107. https://doi.org/10.1016/j.apcata.2009.06.037

16. Kang S-Y, Park C-H, Yoon Y-S et al (2009) Method of extracting butyric acid from a fermented liquid and chemically converting butyric acid into biofuel. Patent from United States https://patents.google.com/patent/US20110294176A1/en

17. Okon E, Shehu H, Gobina E (2018) Novel esterification reaction from biomass product by coupled acetate membrane and catalysts for ethyl lactate separation. Int J Hydrogen Energy 43:7703–7712. https://doi.org/10.1016/j.ijhydene.2017.07.230

18. Saboya RMA, Cecilia JA, García-Sancho C et al (2017) Assessment of commercial resins in the biolubricants production from free fatty acids of castor oil. Catal Today 279:274–285. https://doi.org/10.1016/j.cattod.2016.02.020

19. Xuan W, Hakkarainen M, Odelius K (2019) Levulinic acid as a versatile building block for plasticizer design. ACS Sustain Chem Eng 7:acssuschemeng.9b02439. https://doi.org/10.1021/acssuschemeng.9b02439

20. Liang C, Wang Y, Hu Y et al (2019) Study of a new process for the preparation of butyl levulinate from cellulose. ACS Omega 4:9828–9834. https://doi.org/10.1021/acsomega.9b00735

21. Maheria KC, Lodhi A, Lankapati H, Krishna R (2021) Solid acid-catalyzed esterification of levulinic acid for production of value-added chemicals. In: Pant KK, Gupta SK, Ahmad E (eds) Catalysis for clean energy and environmental sustainability. Springer International Publishing, Cham, pp 345–382

22. Yamada T, Yamaguchi M, Kubo S, Hishikawa Y (2015) Direct production of alkyl levulinates from cellulosic biomass by a single-step acidic solvolysis system at ambient atmospheric pressure. Bioresources 10:4961–4969. https://doi.org/10.15376/biores.10.3.4961-4969

23. Wiseman S, Michelbach CA, Li H, Tomlin AS (2023) Predicting the physical properties of three-component lignocellulose derived advanced biofuel blends using a design of experiments approach. Sustain Energy Fuels 7:5283–5300. https://doi.org/10.1039/D3SE00822C

24. Gallego-Villada LA, Alarcón EA, Romanelli GP (2022) Nanofuel additives. In: Nanotechnology in the automotive industry. Elsevier, pp 561–578. https://doi.org/10.1016/B978-0-323-90524-4.00027-X

25. Morone A, Apte M, Pandey RA (2015) Levulinic acid production from renewable waste resources: bottlenecks, potential remedies, advancements and applications. Renew Sustain Energy Rev 51:548–565. https://doi.org/10.1016/j.rser.2015.06.032

26. Mukesh C, Nikjoo D, Mikkola J-P (2020) Production of C-14 levulinate ester from glucose fermentation liquors catalyzed by acidic ionic liquids in a solvent-free self-biphasic system. ACS Omega 5:4828–4835. https://doi.org/10.1021/acsomega.9b03517

27. Vannice MA (2005) Kinetics of catalytic reactions, 1st edn. Springer US, Boston

28. Ju IB, Lim H-W, Jeon W et al (2011) Kinetic study of catalytic esterification of butyric acid and n-butanol over Dowex 50Wx8-400. Chem Eng J 168:293–302. https://doi.org/10.1016/j.cej.2010.12.086

29. Salvi HM, Yadav GD (2019) Surface functionalization of SBA-15 for immobilization of lipase and its application in synthesis of alkyl levulinates: optimization and kinetics. Biocatal Agric Biotechnol. https://doi.org/10.1016/j.bcab.2019.101038

30. Ahmad E, Khan TS, Alam MI et al (2020) Understanding reaction kinetics, deprotonation and solvation of brønsted acidic protons in heteropolyacid catalyzed synthesis of biorenewable alkyl levulinates. Chem Eng J. https://doi.org/10.1016/j.cej.2020.125916

31. Tian Y, Zhu X, Zhou S et al (2023) Efficient synthesis of alkyl levulinates fuel additives using sulfonic acid functionalized polystyrene coated coal fly ash catalyst. J Bioresour Bioprod 8:198–213. https://doi.org/10.1016/j.jobab.2023.01.003

32. Russo V, Rossano C, Salucci E et al (2020) Intraparticle diffusion model to determine the intrinsic kinetics of ethyl levulinate synthesis promoted by Amberlyst-15. Chem Eng Sci. https://doi.org/10.1016/j.ces.2020.115974

33. Gallego-Villada LA, Alarcón EA, Cerrutti C et al (2023) Levulinic acid esterification with n-butanol over a Preyssler catalyst in a microwave-assisted batch reactor: a kinetic study. Ind Eng Chem Res 62:10915–10929. https://doi.org/10.1021/acs.iecr.3c00893

34. Liu C-H, Chen B-H, Hsueh C-L et al (2009) Hydrogen generation from hydrolysis of sodium borohydride using Ni–Ru nanocomposite as catalysts. Int J Hydrogen Energy 34:2153–2163. https://doi.org/10.1016/j.ijhydene.2008.12.059

35. Sigma-Aldrich (2024) Dowex® 50WX8 hydrogen form, strongly acidic, 50–100 mesh. https://www.sigmaaldrich.com/CO/es/product/sial/44509. Accessed 14 Feb 2024

36. Murzin DYu, Salmi T (2016) Catalytic kinetics: chemistry and engineering, 2nd edn. Elsevier, Amsterdam

37. Fogler HS (2016) Elements of chemical reaction engineering, 5th edn. Prentice Hall, Upper Saddle River

38. Pérez MA, Bringué R, Iborra M et al (2014) Ion exchange resins as catalysts for the liquid-phase dehydration of 1-butanol to di-n-butyl ether. Appl Catal A 482:38–48. https://doi.org/10.1016/j.apcata.2014.05.017

39. Nguyen HC, Ong HC, Pham TTT et al (2020) Microwave-mediated noncatalytic synthesis of ethyl levulinate: a green process for fuel additive production. Int J Energy Res 44:1698–1708. https://doi.org/10.1002/er.4985

40. Ahmad E, Alam MI, Pant KK, Haider MA (2019) Insights into the synthesis of ethyl levulinate under microwave and nonmicrowave heating conditions. Ind Eng Chem Res 58:16055–16064. https://doi.org/10.1021/acs.iecr.9b01137

41. Banchero M, Gozzelino G (2018) A simple pseudo-homogeneous reversible kinetic model for the esterification of different fatty acids with methanol in the presence of Amberlyst-15. Energies (Basel) 11:1843. https://doi.org/10.3390/en11071843

42. Ramkrishna D, Pedro A (1989) Can pseudo-homogeneous reactor models be valid? Chem Eng Sci 44:1949–1966. https://doi.org/10.1016/0009-2509(89)85134-6

43. Zabala S, Reyero I, Campo I et al (2021) Pseudo-homogeneous and heterogeneous kinetic models of the NaOH-catalyzed methanolysis reaction for biodiesel production. Energies (Basel) 14:4192. https://doi.org/10.3390/en14144192

44. Murzin DY, Wärnå J, Haario H, Salmi T (2021) Parameter estimation in kinetic models of complex heterogeneous catalytic reactions using Bayesian statistics. Reac Kinet Mech Cat 133:1–15. https://doi.org/10.1007/s11144-021-01974-1

45. Gallego-Villada LA, Alarcón EA, Palermo V et al (2020) Kinetics for the biodiesel production from lauric acid over Keggin heteropolyacid loaded in silica framework. J Ind Eng Chem 92:109–119. https://doi.org/10.1016/j.jiec.2020.08.030

46. Gallego-Villada LA, Alarcón EA, Ruiz DM, Romanelli GP (2022) Kinetic study of the esterification of t-cinnamic acid over Preyssler structure acid. MolCatal 528:112507. https://doi.org/10.1016/j.mcat.2022.112507

47. Haario H (1994) ModEst user's guide. ProfMath Oy, Helsinki

48. Brooks S, Gelman A, Jones GL, Meng X-L (2011) Handbook of Markov chain Monte Carlo. Chapman & Hall, Boston

49. Ma Y-K, Alomar TS, AlMasoud N et al (2023) Effects of synthesis variables on SAPO-34 crystallization templated using pyridinium supramolecule and its catalytic activity in microwave esterification synthesis of propyl levulinate. Catalysts 13:680. https://doi.org/10.3390/catal13040680

50. Appaturi JN, Selvaraj M, Rajabathar JR et al (2022) Highly efficient non-microwave instant heating synthesis of hexyl levulinate fuel additive enhanced by sulfated nanosilica catalyst. Microporous Mesoporous Mater 331:111645. https://doi.org/10.1016/j.micromeso.2021.111645

51. Escobar AM, Blanco MN, Martínez JJ et al (2019) Biomass derivative valorization using nano core-shell magnetic materials based on Keggin-heteropolyacids: levulinic acid esterification kinetic study with n-butanol. J Nanomater 2019:1–14. https://doi.org/10.1155/2019/5710708

52. Gu H, Jiang Y, Zhou L, Gao J (2011) Reactive extraction and in situ self-catalyzed methanolysis of germinated oilseed for biodiesel production. Energy Environ Sci 4:1337. https://doi.org/10.1039/c0ee00350f

53. Zhou L, He Y, Ma L et al (2018) Conversion of levulinic acid into alkyl levulinates: using lipase immobilized on meso-molding three-dimensional macroporous organosilica as catalyst. Bioresour Technol 247:568–575. https://doi.org/10.1016/j.biortech.2017.08.134

54. Smallwood IM (1996) Handbook of organic solvent properties. Elsevier, Burlington

55. The Engineering ToolBox (2008) Liquids—dielectric constants. https://www.engineeringtoolbox.com/liquid-dielectric-constants-d_1263.html. Accessed 21 Feb 2024

56. Bouguerra Neji S, Trabelsi M, Frikha M (2009) Esterification of fatty acids with short-chain alcohols over commercial acid clays in a semi-continuous reactor. Energies (Basel) 2:1107–1117. https://doi.org/10.3390/en20401107

57. Erdem B, Cebe M (2011) Determination of steric effect on the esterification of different alcohols with propanoic acid over cation-exchange resin catalyst Dowex 50Wx4. Z Phys Chem 225:125–136. https://doi.org/10.1524/zpch.2011.6153

58. Lopes NPG, da Silva MJ (2022) Cesium partially exchanged heteropolyacid salts: efficient solid catalysts to produce bioadditives from the levulinic acid esterification with alkyl alcohols. Reac Kinet Mech Cat 135:3173–3184. https://doi.org/10.1007/s11144-022-02310-x

59. Da Silva MJ, Chaves DM, Teixeira MG, Oliveira Bruziquesi CG (2021) Esterification of levulinic acid over Sn(II) exchanged Keggin heteropolyacid salts: an efficient route to obtain bioaditives. Mol Catal 504:111495. https://doi.org/10.1016/j.mcat.2021.111495

60. Cheng CP (2018) Scale-up of catalyst recipes to commercial production. In: Hoff R (ed) Handbook of transition metal polymerization catalysts. Wiley, Shangai, pp 177–188

61. Yaws CL (2012) Yaw's critical property data for chemical engineers and chemists. Knovel, Norwich

62. Poling BE, Prausnitz JM, O'Connell JP (2000) The properties of gases and liquids, 5th edn. McGraw-Hill, New York

63. Hamryszak Ł, Grzesik M (2021) Kinetics of esterification of the levulinic acid with n-hexanol, n-octanol, and 2-ethylhexanol in the presence of methanesulfonic acid as a catalyst under nonisothermal conditions. Int J Chem Kinet 53:60–66. https://doi.org/10.1002/kin.21425

64. Umrigar V, Chakraborty M, Parikh P (2019) Esterification and ketalization of levulinic acid with desilicated zeolite β and pseudo-homogeneous model for reaction kinetics. Int J Chem Kinet 51:299–308. https://doi.org/10.1002/kin.21253

65. Masuti S, Muto J, Rybacki E (2023) Transient creep of quartz and granulite at high temperature under wet conditions. J Geophys Res Solid Earth 128:1–16. https://doi.org/10.1029/2023JB027762